

## Modelling of combustion and NO<sub>x</sub> emissions in industrial equipment

J.L.T. Azevedo, M.G. Carvalho, P.J. Coelho, C.F.M. Coimbra and M. Nogueira

Instituto Superior Técnico, Technical University of Lisbon, Mechanical Engineering Department,  
Av. Rovisco Pais, 1096-Lisboa codex, Portugal

**Abstract** - The development of industrial boilers and furnaces with higher efficiencies and lower environmental impact, together with the advances in computer power promoted the development of comprehensive models to simulate fluid flow, heat transfer, combustion and pollutant formation. The present paper reviews modelling work performed at Instituto Superior Técnico (IST) concerning the prediction of industrial combustion equipment behaviour and NO emissions. The model is based on the solution of transport equations for momentum, enthalpy, chemical species concentration and turbulent quantities. In the case of coal combustion a Lagrangian description of the particles is considered using a two-way coupling between the particle phase and continuum gas phase. In any case the NO<sub>x</sub> formation is considered in a post-processor routine. The models are applied to gas and oil-fired glass melting furnaces and utility boilers where NO emissions are estimated using the Zeldovich mechanism for thermal-NO. For pulverised coal combustion applications to a single burner furnace and to a multi-burner boiler are described and NO emissions are estimated using the De Soete reaction mechanism for fuel-NO.

### INTRODUCTION

The fuel resources limitations and the pollution problem awareness motivated the researchers on industrial process furnaces and boilers to improve efficiency and reduce pollutants emissions. Advances in computer power allied to advances in the understanding of fluid mechanics promoted the application of computational fluid dynamics to the analysis of combustion equipment for the last two decades. The computer codes incorporate adequate physical models required to allow the evaluation of all relevant phenomena occurring in the combustion chambers. These codes are substituting global and zonal models with the advantage of coupling the calculation of fluid flow, combustion and heat and mass transfer. The flexibility of these models is clearly demonstrated by their application to utility boilers and industrial furnaces. Recent reviews of these developments are available.<sup>1-2</sup>

In today's research, particularly acute is the need to comply with more stringent ecological requirements, by lowering the noxious gas emission without sacrificing production. The large amount of air preheat and the elevated flame temperature in many gas and oil furnaces yield high levels of thermal NO<sub>x</sub> emissions which are causing concern. Also the necessity to use lower quality coals with considerable nitrogen and sulphur content increases the harmful emissions. Reductions in NO<sub>x</sub> emissions are achievable through combustion modifications, but parametric trials on full scale equipment are very expensive and accurate measurements are difficult to obtain. Hence, mathematical models are a valuable tool to help engineers in the struggle for reduction of pollutants emission.

A brief review of the NO<sub>x</sub> modelling in practical systems may be found in Ref. 3. Since the present work describes applications to utility boilers and glass furnaces only previous work dedicated to such equipment is mentioned here. The prediction of NO<sub>x</sub> emissions in glass furnaces is based on the use of the Zeldovich mechanism describing thermal NO formation. The inverse reactions of the Zeldovich mechanism which are often neglected in other applications have been found to be important in glass furnaces due to the high temperatures achieved<sup>3-4</sup>. A similar thermal NO formation model has been applied to oil-fired utility boilers<sup>5-6</sup>. A more complex model based on a detailed reaction mechanism and finite rate chemical kinetics was employed in Ref.7. For coal-fired boilers the main source of NO is the nitrogen content of the fuel and the NO emission is described by the De Soete mechanism<sup>8</sup>. Several applications to coal-fired boilers have recently appeared in the literature<sup>9-11</sup>.

The objective of this paper is to describe models of thermal and fuel NO formation and present the work carried out at Instituto Superior Técnico which is part of the Technical University of Lisbon concerned with the application of such models to utility boilers and glass furnaces. In this paper, the next section describes the models used to calculate NO emissions. The following

section describes applications to glass melting furnaces and utility boilers. A small furnace with a single pulverised coal burner is also considered to test the combustion and fuel NO model. The last section presents some general concluding remarks of the present work.

## MATHEMATICAL AND PHYSICAL MODELS

### Turbulence, combustion and radiation models

The mathematical modelling of industrial combustion chambers is based on the numerical solution of the governing Favre-averaged conservation equations for a turbulent high Reynolds number flow. The mean flow equations are closed by the  $k$ - $\epsilon$  eddy viscosity/diffusivity model which comprises transport equations for the turbulent kinetic energy, its dissipation rate, and constitutive relations for the Reynolds stresses and turbulent scalar fluxes.

Combustion in gas flames is modelled assuming a simple chemically reacting system (SCRS). This model is based on the following assumptions: the reaction rates associated with the fuel oxidation have very small time scales compared with those characteristics of the transport phenomena and so chemical reactions take place instantaneously as soon as the reactants are brought together; the mass diffusion coefficients of all chemical species and the thermal diffusion are equal; the reaction between the fuel and the oxidant can be represented by a global one step reaction. These hypotheses allow the calculation of the instantaneous mass fraction of the chemical species as a function of a strictly conserved scalar variable often taken as the mixture fraction.

In a turbulent flow the mixture fraction fluctuates and knowledge of its mean value is insufficient to allow the calculation of the mean values of chemical species mass fractions, temperature and density. The fluctuating nature of the reactive flow may be accommodated through an assumed probability density function (pdf) for the mixture fraction. A clipped Gaussian distribution or a beta pdf are the most common assumptions. These pdfs are completely defined by the mean value and variance of the mixture fraction.

In the case of pulverised coal combustion, instead of considering a mixture fraction, transport equations are solved for the oxidant, volatile and combustion products. Combustion of the volatiles in the gas phase is supposed to be controlled by a turbulent mixing rate using the eddy dissipation model<sup>12</sup> and a chemical kinetic rate of volatiles<sup>13</sup>. The combustion rate is calculated by parallel competition of the two rates<sup>14</sup>. The volatiles mass sources are a result of the computation of the coal particles evolution by tracking representative particles in the flow domain.

The particle momentum equation is analytically integrated in time steps dictated by the grid dimensions and by turbulence. The interaction of a given eddy with the particle trajectory is limited in time by the eddy lifetime and the time for a particle to cross an eddy<sup>15</sup>. The temperature of the particle is calculated from the energy balance equation solved along trajectories. Particle drying, devolatilization and char burnout are considered in sequence<sup>14</sup>. Devolatilization is handled by a first order kinetic rate<sup>16</sup> and the char combustion rate is a combination of diffusion and kinetic rates<sup>17</sup>.

The use of representative particles requires a large number of coal particles to be tracked to achieve statistical independent source terms of volatiles, combustion products and oxygen. In the calculations presented here, about 2000 different trajectories were calculated for each call of the Lagrangian routine. This routine was called each 20 to 50 iterations of the flow field computation and a carefully chosen criterion of accumulating the contributions of trajectories computed in different iterations was considered for the three dimensional case<sup>18</sup>.

The radiative heat transfer is calculated using the discrete transfer method<sup>19</sup>. This method is based on the direct solution of the radiation intensity transport equation. The absorption coefficient of the medium is calculated using the mixed grey and clear gas formulation<sup>20</sup>, extended to account for soot. In the case of pulverised coal combustion, the particle emissivities are calculated according to ref. 21.

Soot is of concern because its presence greatly augments the radiation heat transfer and because it is a pollutant. A simple global expression similar to that used in ref. 22 may be used to calculate soot production. Soot oxidation is modelled following the method outlined in ref. 12.

### NO<sub>x</sub> model

The major part of NO<sub>x</sub> in practical systems has been found to be NO. Consequently, the large amount of theoretical and experimental studies have been focused on NO formation. Nitric oxide may be built up from different reactions paths. The importance of each path depends on the combustion condition. Thermal NO refers to NO obtained from oxidation of molecular nitrogen from air, while fuel NO designates NO formed from oxidation of nitrogen bounded in the fuel.

A third mechanism for NO formation is termed prompt NO. The importance of this last mechanism in flames with excess air is smaller than the others which are treated in this work. The prompt NO was proposed to explain observed excess of NO formation in the vicinity of the combustion zone. This rapidly formed NO is supposed to accumulate from reactions between nitrogen and CH radicals followed by oxidation which is similar to the mechanisms proposed for fuel NO.

As NO is present only in trace amounts and it has negligible influence on the heat release and on the temperature field, its calculation has traditionally been considered to be independent of the combustion and aerodynamics calculation.

**Thermal NO.** At high temperatures the thermal NO builds up by reactions that are slow enough to be controlled by chemical kinetics. Thus, the modelling of NO formation presumes a finite reaction rate and the assumption of chemical equilibrium made for the combustion model is not valid here.

The kinetic route of NO formation is not the direct reaction between oxygen and nitrogen molecules ( $N_2 + O_2 \rightleftharpoons 2NO$ ) and therefore the presence of atoms and radicals has to be considered. Oxygen atoms are formed from dissociation of  $O_2$  or from the hydrogen atom attack on  $O_2$ . The oxygen atoms that are formed will then attack the nitrogen molecules along the Zeldovich mechanism:



From the Zeldovich mechanism and assuming steady state for the nitrogen atom concentration, the relation giving the NO production rate can be determined as a function of the rate constants of the direct and reverse reactions. The form of the production rate can be further simplified assuming the reaction between the N and OH radicals to be negligible and partial equilibrium for the reactions of the oxygen atom formation (see, e. g., ref. 4) yielding:

$$\frac{d[NO]}{dt} = \frac{2[O] \left( K_A K_B [O_2] [N_2] - K_{-A} K_{-B} [NO]^2 \right)}{K_B [O_2] + K_{-A} [NO]} \quad (1)$$

Where  $K_A$  and  $K_B$  denote the forward constant rates of reactions (RA) and (RB) of the Zeldovich mechanism and  $K_{-A}$  and  $K_{-B}$  stand for the reverse reactions. The concentration of the oxygen atom is calculated from partial equilibrium of oxygen dissociation:

$$[O] = [K_v [O_2]]^{0.5} \quad (2)$$

The values  $K_A$ ,  $K_B$ ,  $K_{-A}$ ,  $K_{-B}$  and  $K_v$  were taken from data published by Baulch *et al.*<sup>23</sup>

Equation (1) has been used in this work to model the NO formation rate. The time-mean NO mass concentration is calculated from its transport equation whose source term is computed from equation (1). Note that in most of the previous studies the reverse reactions of the Zeldovich mechanism were not taken into account. Ignoring these reactions results in overestimation of the NO emissions for the glass melting furnaces.

**Fuel NO.** The main gas species containing nitrogen produced during coal evolution are HCN and  $NH_3$ . Once the fuel nitrogen is converted to HCN it rapidly decays to  $NH_3$  which react to form NO and  $N_2$ . Recognizing the importance of HCN as a precursor to the subsequent nitrogen compound intermediates, De Soete<sup>8</sup> correlated the rate of NO formation and decay with a pair of competitive parallel reactions, each first order in HCN, which represents the pool of nitrogen containing species:

$$R_{HCN \rightarrow NO} = 10^{10} \rho X_{HCN} X_{O_2}^b e^{-33700/T} \quad \text{kg/m}^3 \text{ s} \quad (3)$$

$$R_{NO \rightarrow N_2} = 3 \times 10^{12} \rho X_{HCN} X_{NO} e^{-30000/T} \quad \text{kg/m}^3 \text{ s} \quad (4)$$

X represents mole fractions of the chemical species and b is the order of reaction for molecular oxygen which is a function of oxygen concentration. The two reaction rates are included in transport equations for HCN and NO and form the basis for the fuel NO post processor which allows the calculation of NO formation for pulverised coal flames. The heterogeneous reduction of NO by char based on the kinetic rate of ref. 24 was found to have a minor influence on a single burner test study<sup>25</sup> and thus it was not considered. The thermal NO mechanism was not considered for the pulverised coal applications, although it can be incorporated in the NO transport equation.

## APPLICATIONS OF THE MATHEMATICAL MODEL

In the present section, results obtained using the models described in the previous section are presented for different combustion chambers. The section is divided into three parts. The first part is dedicated to glass furnaces, the second part considers an oil-fired boiler and the last part presents results for pulverised coal combustion. The numerical studies performed are applications to Portuguese industrial equipment.

### Glass melting furnace

The model has already been applied to several furnaces and the most relevant results are published in the literature. In Ref.26 a combined numerical and experimental study was conducted to improve combustion conditions, burners geometry and validate the model. The model for thermal NO was applied for the first time to a cross-fired regenerative glass melting furnace in the work described in Ref. 4. Parametric studies were performed for another cross-fired regenerative furnace with similar geometry but consisting of only four rows of ports<sup>3</sup>.

Recently, Carvalho and Nogueira<sup>27</sup> presented a study of an end-port glass furnace aimed at an integrated evaluation of the effect of changes in the operating conditions on the furnace performance, as a basis for future development of automatic advising devices. The studied furnace is used to produce glass containers. The predictions have been obtained for the following standard operating conditions: fuel mass flow rate=0.17 kg/s, air/fuel ratio=17 kg<sub>air</sub>/kg<sub>fuel</sub>, white glass.

The furnace geometry is shown in figure 1 and the predicted flow pattern is sketched in figure 2. These predictions were obtained by using three-dimensional modelling procedures for the whole furnace system, heating chamber and load.

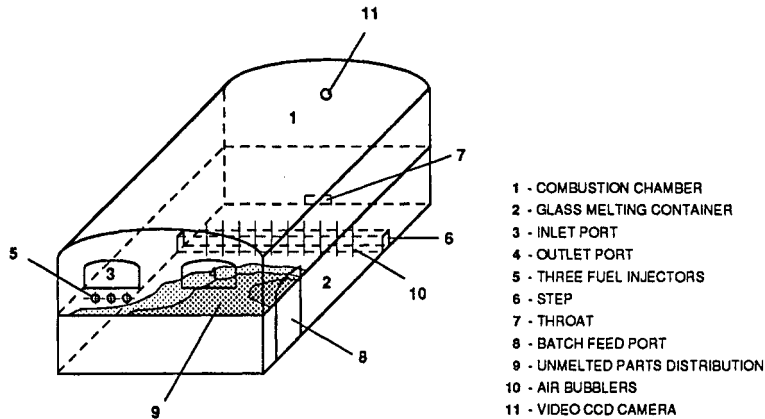


Figure 1 - Sketch of the end-port glass furnace.

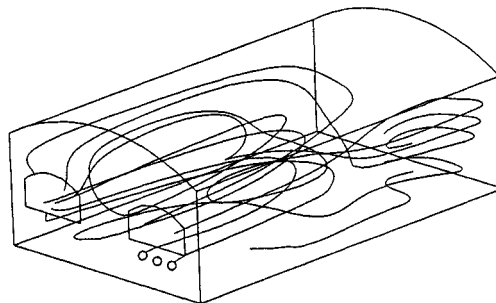


Figure 2 - Flow pattern inside the combustion chamber.

Figure 3 shows the NO mass fraction in horizontal and vertical planes crossing the burners location. It can be seen that several local concentration peaks are present. This is due to the presence of critical temperature combined with oxygen and nitrogen concentrations in different locations. The attenuation of those peaks may be accomplished changing the operating conditions and the flame shape in order to try to achieve a more uniform temperature distribution.

The formation of NO is strongly influenced by the presence of high local gas temperatures and significant NO reduction may occur when the reaction products are at intermediate temperature levels. At this temperature range, the equilibrium NO concentration is smaller and the reaction rate of the Zeldovich mechanism is still significant. Coupling both possibilities — to attenuate temperature peaks and to increase the residence time of the combustion products at intermediate temperatures — it is possible to decrease significantly the NO emissions. However, a combination of both aspects is not possible in all thermal equipments due to technological limitations. The reduction of NO emissions will be effective in a combustion chamber where the flame is long, the temperature distribution is smooth and the combustion products stay inside the chamber during a significant time.

Fortunately, in glass melting furnaces these ideal conditions may be approached. Significant temperature peaks do not generally occur due to the structural limitations and large dimensions of the glass-melting tank. The flame has to be long and the gas temperature should be as uniform as possible. In the end-port furnaces — the more common glass furnace geometry — combustion gases stay inside the combustion chamber for a long period. This high residence time is due to the loop formed by

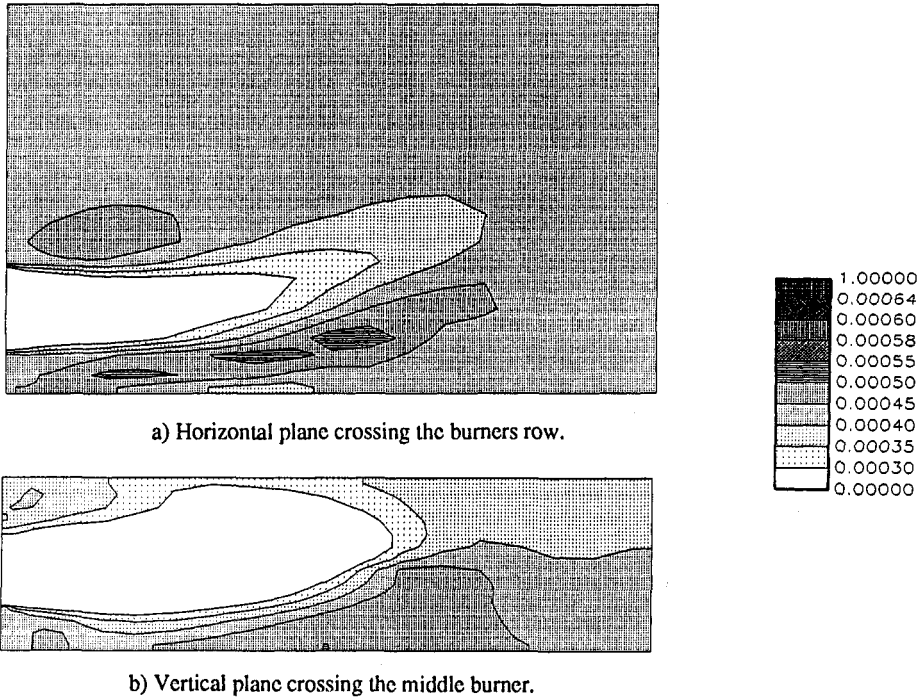


Figure 3 - NO mass fraction distribution inside the combustion chamber.

the gas flow inside the combustion chamber. This horseshoe flow pattern is imposed by the location of burners, secondary air entrance and outlet port in the same furnace wall. This configuration is used to allow the regenerative heat recovery and the correspondent cyclical working mode. Thus, in glass furnaces, and particularly for end-port furnaces, it is possible a significant reduction of the NO<sub>x</sub> emissions by adjusting the geometric parameters and operating conditions that control the flame shape, the temperature distribution and the gas residence time.

**Oil-fired boiler**

The study of a power station boiler of the Portuguese Electricity Utility is reported in this section. It is a natural circulation drum boiler with a pressurized combustion chamber, parallel passages by the convection zone and preheating. It is prepared for out-door installation and fuel oil burning, being easily adapted to natural gas and fuel oil/natural gas burning. Vaporization of the fuel was assumed to occur instantaneously. The boiler is fired from three levels of four burners each, placed on the front wall. A simplified sketch of the combustion chamber is presented in figure 4. At maximum capacity (771 t/h at 167 bar and 545 °C) the fuel mass flow rate is 15.8 kg/s, the air mass flow rate is 238.7 kg/s and the output power is 250 MWe.

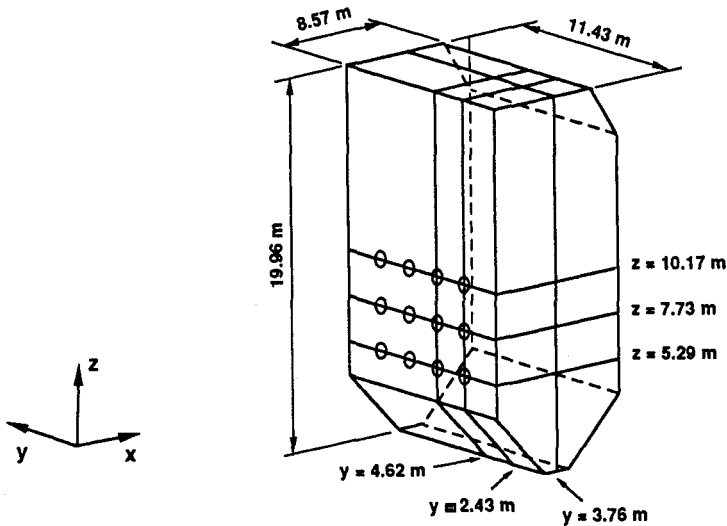


Figure 4 - Sketch of the oil-fired boiler.

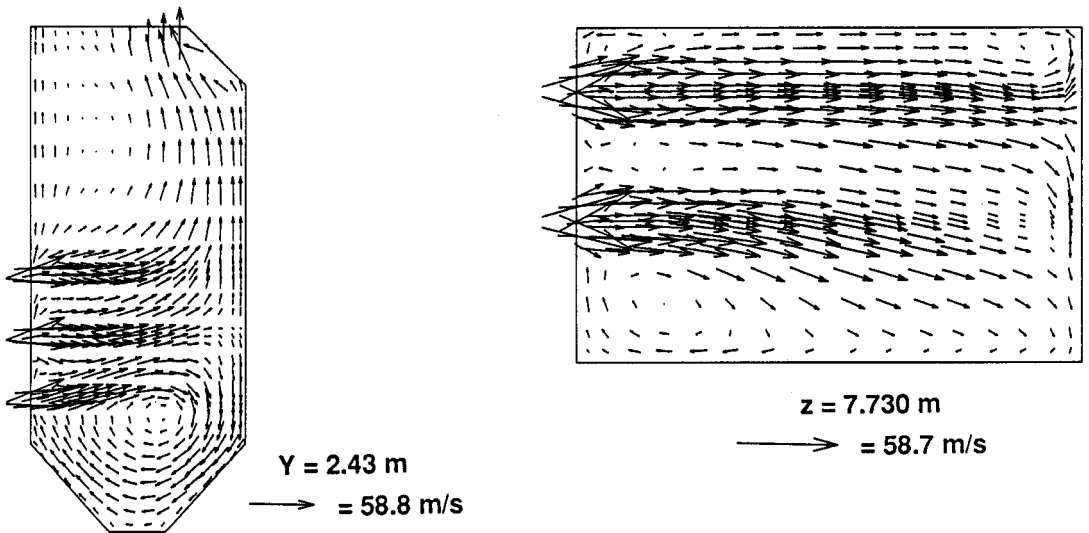


Figure 5 - Predicted velocity field.

Predictions of the velocity field in a horizontal plane crossing the second level of burners is presented in figure 5. The upper boundary of the plot is coincident with the symmetry axis of the boiler and, therefore, only two of the burners are visible. The flow close to the burners is rather complex due to the swirl of the combustion air. Analysis of the flow field reveals that the horizontal velocity component decreases towards the back wall of the boiler. This effect is more pronounced for the low level of burners (not shown here) due to the flow deflection towards the ash-pit where a large vortex is formed. Consequently, the mean residence time of the fuel introduced through the burners at the lower level is much higher than for the fuel introduced through the burners at higher levels. Close to the back wall and above the burners level a region of low velocities is present. This phenomenon is a consequence of the high velocity of the inlet air that moves towards the back wall and collides with it overweighing the momentum turbulent diffusion.

The gas temperature distribution (see figure 6) denotes high gradients near the burners especially in the flame front region where combustion takes place. The temperature increases as the distance from the burners increases and combustion progresses. At the two top levels of burners the temperature achieves the highest values around 1900 K and above 2000 K in a small region. These temperatures are achieved at a distance between 2 and 3 m of the front wall and they do not change significantly up to the back wall. The turbulence/combustion interaction tends to homogenize the temperature by lowering the peak levels that would occur otherwise. In the ash-pit and above the top level of burners the gas temperature decreases due to the heat loss by radiation to the wall. As the combustion products approach the exit section the temperatures become more homogenous.

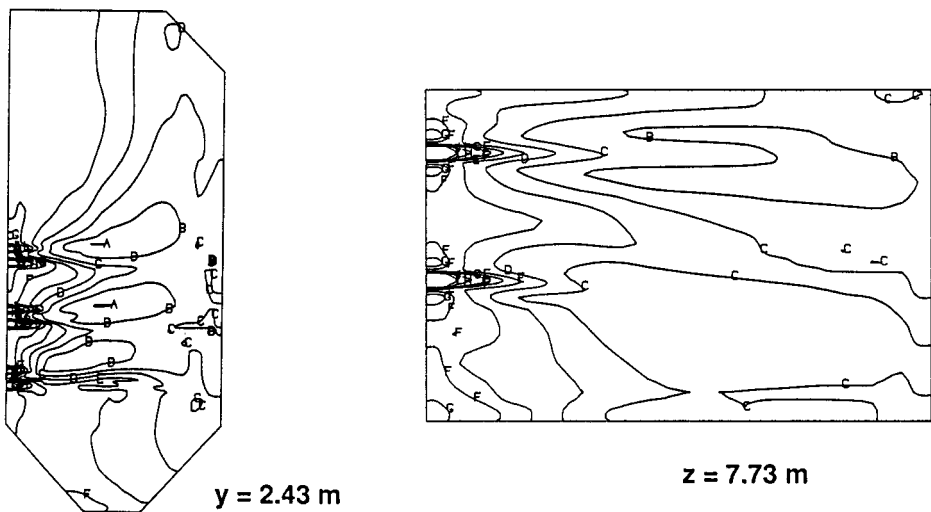


Figure 6 - Predicted temperature contours (K). (A-2000, B-1900, C-1800, D-1700, E-1600, F-1500, G-1400, H-1200, I-1000)

The predicted thermal NO distribution normalized by the maximum predicted value is presented in figure 7. Higher production rates occur in the lean - fuel side of the flame front where the temperatures are high and the oxygen concentration is significant. In regions where the concentration of NO is significant, the temperature exceed 1400K and there is oxygen available, NO oxidation takes place and may dominate its formation. These considerations explain the predicted distribution: NO concentration increases from the burners as long as combustion takes place. When combustion finishes the temperatures are high enough for the inverse reactions of the Zeldovich mechanism to occur and since there is oxygen available the NO concentration decreases. However, the NO distribution does not change between a few meters above the burners level and the exit to the superheaters suggesting that the reactions involving NO formation or oxidation are no longer significant. The predicted average value at the exit is below the range expected. This underestimation may be explained by the formation of NO which was not accounted for, namely some contribution from the nitrogen contained in the fuel oil.

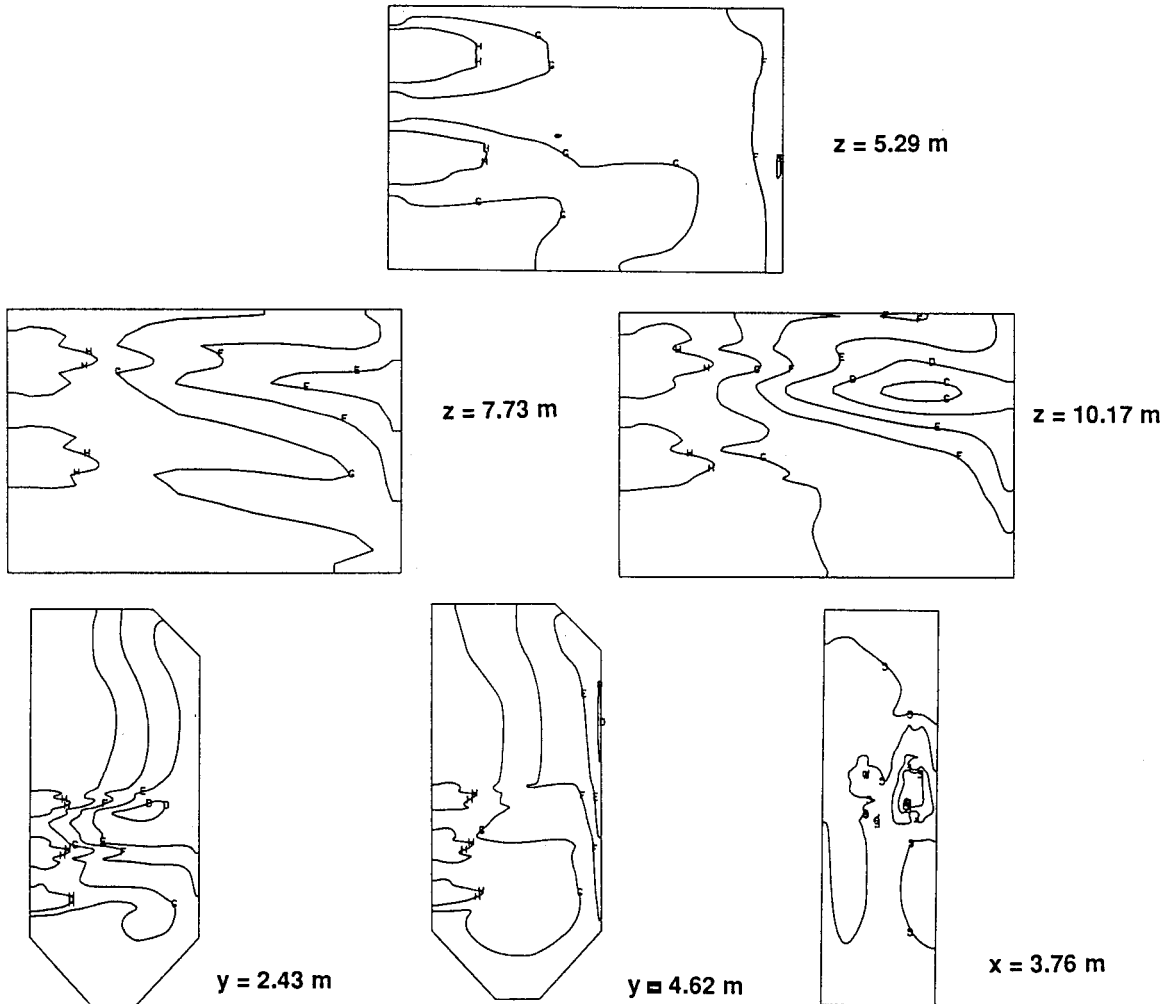


Figure 7 - Predicted NO mass fractions normalized by the maximum value (A-1.00, B-0.875, C-0.75, D-0.625, E-0.50, F-0.375, G-0.25, H-0.125).

### Pulverised coal flames

The pulverised coal study was concerned both with axisymmetrical single burner furnace and a utility boiler. The axisymmetrical case was used to test and develop a numerical model considering the lagrangian description of the coal particles and the fuel NO model. The model was then applied to a three dimensional geometry corresponding to a utility boiler 300 MWe equipped with 20 burners.

The axisymmetrical study was based on the experimental results obtained in the downward fired cylindrical furnace of 0.6 m in diameter installed at Imperial College of London.<sup>28-29</sup> The operating conditions considered in the present work correspond to a swirl number of 1.43 and excess air level of 15%.

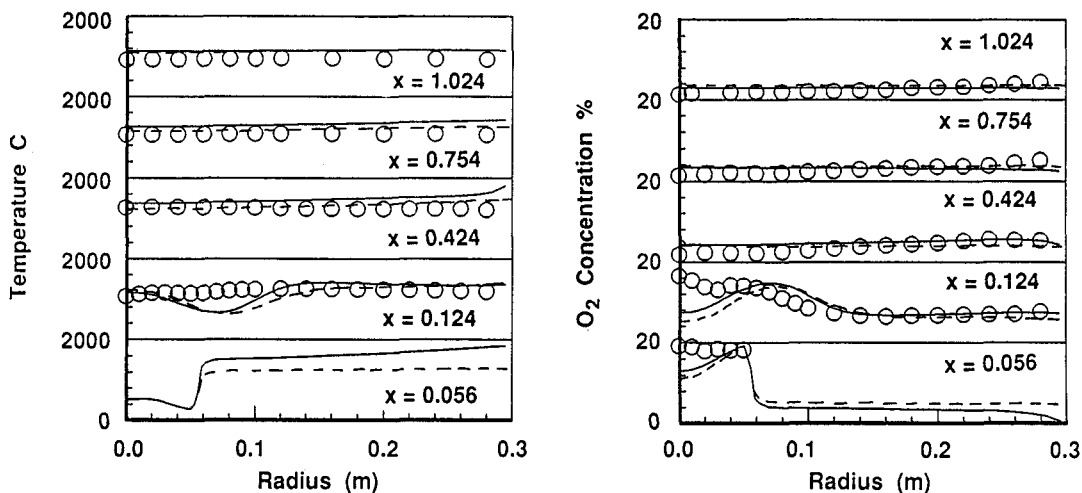


Figure 8 - Radial profiles of a) Oxygen concentration, b) Temperature.

Figures 8a) and 8b) show the comparison of the model predictions with experimental results of oxygen concentration and temperature radial profiles for different axial positions along the furnace. The figure shows a predicted early oxygen consumption close to the burner which was observed to be the result of particles being reversed in the central recirculation zone and burning close to the burner quart. The two curves in each figure correspond to two different kinetic rates of char combustion. The full line corresponds to a slower kinetic rate and thus smaller oxygen consumption close to the burner in better agreement with experimental results. The second axial position suggests that the proximity of the internal recirculation zone is overpredicted by the model. The oxygen consumption in the external recirculation zone is similar for both kinetic rates. For lower swirl<sup>14,25</sup>, the extension of the external recirculation zone is smaller and the amount of combustion in these zone is very sensitive to the kinetic rate of char burnout. The predicted temperature profiles show a reasonable good agreement except close to the beginning of the internal recirculation zone.

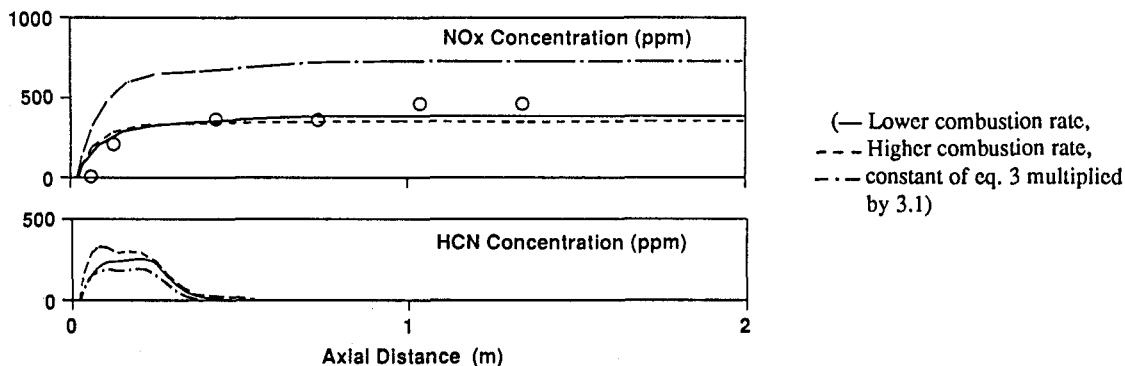


Figure 9 - Centreline HCN and NO concentrations.

Figure 9 shows the HCN and NO axial concentration profiles for the two reaction rates considered using the constant presented in equation 3 and this constant multiplied by 3.1 using the lower reaction rate. Although the kinetic rate of coal combustion influences the HCN profile the NO formed is little affected. The oxidation rate constant increased has been used by different authors in literature<sup>9</sup> but in the present model predictions the original constant performs better. This is not the case for the industrial scale study discussed below where a constant an order of magnitude larger gave the best results. The agreement with the experimental measurements considered show a small increase of NO emission with swirl although earlier results obtained in the same furnace showed the opposite behaviour. The NO emissions present a minimum value close to the swirl number considered here.

The numerical techniques previously developed to the prediction of the 2-D axisymmetrical pulverised coal burners were adopted to describe an industrial pulverised-fuelled boiler (group 3 of the Sines Power Plant of Portugal). Figure 10 presents the cross section of the studied combustor which contains five levels of burners. The lateral side of the boiler (not shown in this figure) is 15. m width and includes four rows of burners. The three-dimensional code simulates numerically the combustion, heat transfer and flow field of the reactive two-phase flow in half of the boiler, assuming symmetry by considering that the influence of swirl is only significative close to the burners.



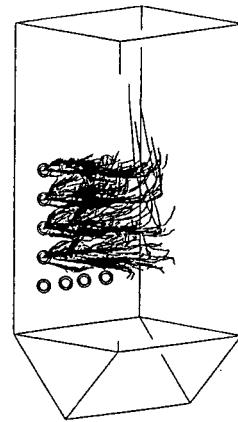
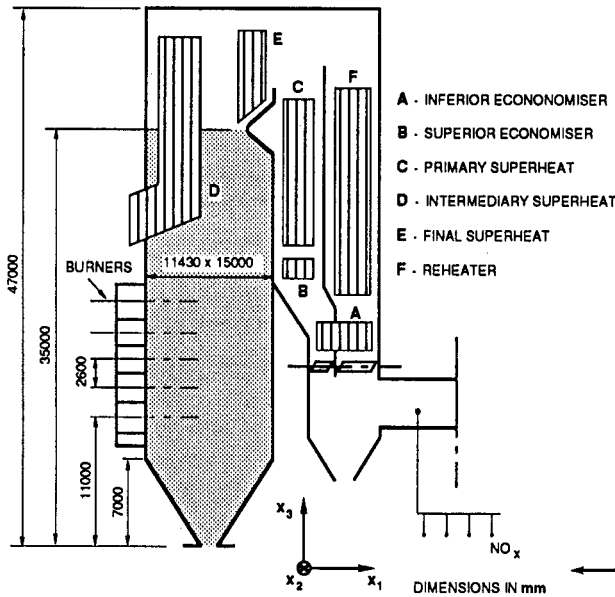


Figure 11 - Representative trajectories of the coal particles.

Figure 10 - Geometry of the coal fired boiler.

Figure 11 shows representative trajectories of the coal particles here calculated with the aid of special strategy of particle dispersion<sup>18</sup>. The operating conditions correspondent to this figure is a result of the BOOS (Burners-out-of-Service) technique applied to reduce the overall NO emissions from this boiler. The sensitivity of the fully three-dimensional model was found very satisfactory for several different operating cases when compared with the measurements of NO concentrations performed in the flue gases of the furnace<sup>11</sup>. The measured values of NO emissions remain roughly in the range of 600 to 660 ppm (6% O<sub>2</sub>) where the smaller values are related to successful applications of the BOOS techniques for the first or fifth rows of burners leading to the expected reductions. The calculated values are slightly overpredicted using a constant an order of magnitude larger for the pre-exponential constant of the DeSoete's mechanism. The values obtained with the model vary between 620 to 723 ppm (6% O<sub>2</sub>) for all operating cases studied. The sensitivity to changes in key-variables such as the particle averaged diameter is also stimulant, where predicted values shifted by less than 5% of absolute measured values were found.

Figure 12a) shows the temperature values of the normal operation for a vertical plane containing the burners centrelines. Figure 12 b) and c) are related to the distributions of oxygen and NO for the same operating case, respectively. The scale of figure 12 c) was selected in that range to show the rapid formation of NO due the oxidation of HCN in the envelop of the flames. The flames shape can be identified by temperature and oxygen distribution which is the result of the char burnout and volatiles combustion in both particulate and gaseous phase.

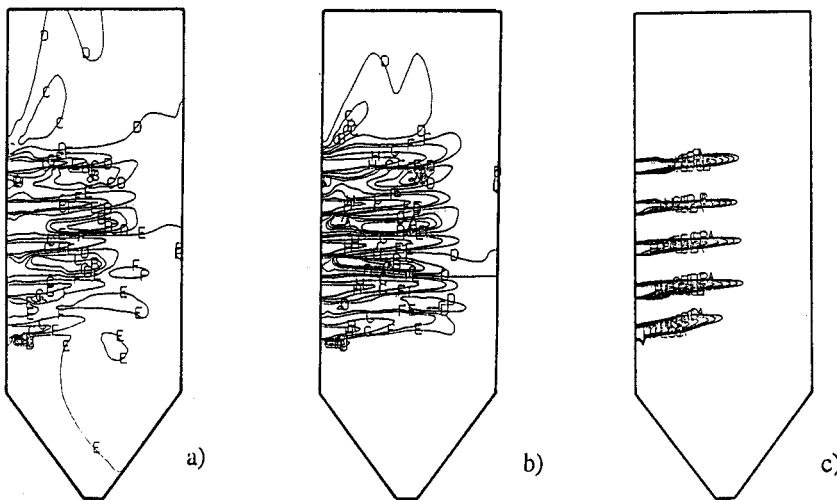


Figure 12 - Predicted values in the coal fired boiler

- a) Temperatures (K) - (A-2500, B-2250, C-2000, D-1750, E-1400, F-1000, G-700).
- b) Oxygen mass fractions (%). (A-1, B-2, C-3, D-4, E- 8, F-10, G-15, H-20).
- c) NO mass fractions (ppm). (A-400, B-350, C-300, D-250, E-200, F-150, G-100, H-50).

## CONCLUSIONS AND FINAL REMARKS

A three dimensional mathematical model was developed to predict the behaviour of combustion chambers of industrial equipment burning gas, oil or coal. The complete validation of three dimensional models is scarce due to the difficulties in obtaining experimental results but the comparisons performed so far are encouraging. The use of simpler geometries to perform detailed comparison with experimental results is a way to support the developments of the three dimensional models.

The predicted NO emissions from glass furnaces are in reasonable agreement with experimental measurements but in the oil-fired boiler the predicted values are lower than the measured ones. This is probably due to a significant contribution from nitrogen in the fuel oil which was neglected in the present analysis.

The prediction of axisymmetric pulverised coal flames shows the influence of some inaccuracies in the turbulence model. The application of the model to a coal-fired boiler, although requiring fitting of a model constant in accordance with other authors, has shown the ability to predict the influence of operating conditions on the NO emissions.

It can be concluded that the use of three-dimensional mathematical models is a real alternative to predict and evaluate the effect of changes in operating conditions and design parameters on the pollutant emissions. The so-called secondary measures may represent an important reduction on the NO pollutant emissions in industrial equipments.

## REFERENCES

1. Meunier, H., Proc. 2nd European Conference on Industrial Furnaces and Boilers, Vilamoura, Portugal, 2-5 April (1991).
2. Carvalho, M.G., Coelho, P.J. and Nogueira, M., Proc. 1st European Thermal Sciences and 3rd UK National Heat Transfer Conference, University of Birmingham, United Kingdom, 16-18 September (1992).
3. Carvalho, M.G., Semião, V.S. and Coelho, P.J., to appear in ASME J. Engineering for Industry (1992).
4. Carvalho, M.G., Semião, V., Lockwood, F.C. and Papadopoulos, C., Journal of the Institute of Energy, 39-47 (1990).
5. Carvalho, M.G., Coelho, P.J. and Costa, F., Proc. 2nd European Conference on Industrial Furnaces and Boilers, Vilamoura, Portugal, 2-5 April (1991).
6. Bonvini, M., Piana, C. and Vigevano, L., 1st Int. Conference on Combustion Technologies for a Clean Environment, Vilamoura, Portugal, 3-6 September (1991).
7. De Michele, G., Pasini, S. and Tozzi, A., Proc. 2nd European Conference on Industrial Furnaces and Boilers, Vilamoura, Portugal, 2-5 April (1991).
8. De'Soete, G.G., 15th Symp. (Int.) on Combustion, p. 1093, The Combustion Institute (1975).
9. Fiveland, W.A., Wessel, R.A. and Eskinazi, D., 24th Nat. Heat Transfer Conference, Pittsburgh (1987).
10. Gormer, K. and Zinser, W., ASME 107th Winter Annual Meeting, California, USA, 7-12 December (1986).
11. Coimbra, C.F., Azevedo, J.L.T. and Carvalho, M.G., Submitted to Combustion Science & Technology (1992).
12. Magnussen, B.F. and Hjertager, B.H., 16th Symp. (Int.) on Combustion, p. 719, The Combustion Institute (1977).
13. Shaw, D.W., Zhu, X., Misra, M.K. and Essenhigh, R.H., 23rd Symp. (Int.) on Combustion, p. 1152, The Combustion Institute (1990).
14. Azevedo, J.L.T. and Carvalho, M.G., 1st Int. Conference on Combustion Technologies for a Clean Environment, Vilamoura, Portugal, 3-6 September (1991).
15. Azevedo, J.L.T. and Pereira J.C.F., Particle and Particle Systems Characterization, 7, 171-180 (1990).
16. Badzioch, S. and Hawkesley, P.G.W., Ind. Eng. Chem. Process Des. Dev., 9(4), 521-530 (1970).
17. Field, M.A., Combustion and Flame 14, 237-248 (1970).
18. Coimbra, C.F. and Carvalho, M.G., 4th Brazilian Thermal Science Meeting, Rio de Janeiro, Brazil, 2-4 December (1992).
19. Lockwood, F.C. and Shah, N.G., 18th Symp. (Int.) on Combustion, p. 1405, The Combustion Institute (1981).
20. Hottel, H.C. and Sarofim, A.F., Radiative Transfer, McGraw-Hill, New York (1967).
21. Baum, M.M. and Street, P.J., Combustion Science and Technology, 3, 231-243 (1971).
22. Khan, I.M. and Greeves, G.A., Heat Transfer in Flames, p. 391, (Ed. Afgan and Beer) (1974).
23. Baulch, D.L., Drysdale, D.D., Horne, D.G. and Lloyd, A.C. Evaluated kinetic data for high temperature reactions (3 vol.), Butterworth Editors, CRC Press, United Kingdom (1973).
24. Levy, J.M., Chan, L.K., Sarofim, A.F. and Béér, J.M., 18th Symp. (Int.) on Combustion, p. 111, The Combustion Institute (1981).
25. Azevedo, J.L.T. and Carvalho, M.G., 6th Workshop on Two-Phase Flow Predictions, Erlangen, Germany, 30 March - 2 April (1992).
26. Carvalho, M.G., Durão, D.F.G. and Pereira J.C.F., Eng. Comput. 4, 23-34 (1987).
27. Carvalho, M.G. and Nogueira, M., E.S.G.Conf. on the Fundamental of the Glass Manufacturing Process, Sheffield, U.K., September (1992).
28. Abbas, T., Costen, M., Costen, P. and Lockwood, F.C., Combustion and Flame 87, 104-108 (1991).
29. Godoy, S., Ismail, M. and Lockwood, F.C., Comb. Sci. and Tech. 67, 59-72 (1989).